Neuron, Vol. 23, 325–335, June, 1999, Copyright ©1999 by Cell Press

Laser Ablations Reveal Functional Relationships of Segmental Hindbrain Neurons in Zebrafish

Katharine S. Liu and Joseph R. Fetcho*
Department of Neurobiology and Behavior
State University of New York at Stony Brook
Stony Brook, New York 11794

Summary

Segmentation of the vertebrate brain is most obvious in the hindbrain, where successive segments contain repeated neuronal types. One such set of three repeated reticulospinal neurons—the Mauthner cell, MiD2cm, and MiD3cm—is thought to produce different forms of the escape response that fish use to avoid predators. We used laser ablations in larval zebrafish to test the hypothesis that these segmental hindbrain cells form a functional group. Killing all three cells eliminated short-latency, high-performance escape responses to both head- and tail-directed stimuli. Killing just the Mauthner cell affected escapes from tail-directed but not from head-directed stimuli. These results reveal the contributions of one set of reticulospinal neurons to behavior and support the idea that serially repeated hindbrain neurons form functional groups.

Introduction

A striking feature of the vertebrate brain is its division into segments that are recognizable at all levels of organization, from the gross anatomical to the molecular. This segmentation is most evident in the hindbrain, which contains reticulospinal neurons whose axons project into spinal cord to influence spinal circuits involved in motor control. Successive hindbrain segments contain morphologically similar reticulospinal neurons that form serially repeated arrays of cells. Even though serially homologous neurons are present in the hindbrain of diverse vertebrates, little is known about their contributions to behavior.

In larval zebrafish, where the small number of neurons allows the identification of individual cells, one can recognize single, morphologically similar cells in successive hindbrain segments (Kimmel et al., 1982; Metcalfe et al., 1986). One such set includes three bilateral pairs of neurons in adjoining segments—the Mauthner cell in hindbrain segment 4 and two serial homologs, MiD2cm and MiD3cm, located in successive segments caudal to the Mauthner cell. The neurons in this set are thought to generate an escape behavior used by fish to avoid predators. When presented with a threatening stimulus, a fish responds with a characteristic fast turn away from the stimulus that allows the animal to swim off in the direction opposite the threat. This highly reproducible, extremely fast escape response, also known as the fast-start response, is essential to the survival of the animal. As reproducible as the behavior is, it is also modifiable. Responses are directional, with the magnitude of the turn depending upon the location of the stimulus (Eaton et al., 1984; Eaton and Emberley, 1991). Thus, the circuitry that mediates successful escape responses provides not only short latency and high speed but also proper timing and direction of movement.

The Mauthner cells are thought to be involved in the initiation and laterality of the escape response. There is a one-to-one correspondence between the Mauthner cell firing and subsequent expression of the fast-start response (Zottoli, 1977; Eaton et al., 1981), supporting the cell's role in the initiation of escape. The laterality of the initial turn of the escape response is thought to be determined by which of the two Mauthner cells is activated (Eaton and Kimmel, 1980). A large sensory input on one side of the fish leads to activation of the Mauthner cell on that side. Because the Mauthner axon crosses the midline to excite axial motoneurons on the opposite side, activation of the Mauthner cell causes a turn away from the stimulus.

The existence of a bilateral pair of Mauthner cells might explain how lateral directionality of escape is mediated but is not sufficient to account for the varied directionality of observed turns. Direct electrical stimulation of the Mauthner cell in unrestrained goldfish results in weaker and less variable responses than sensory-evoked responses (Nissanov et al., 1990), suggesting that the Mauthner cell cannot, by itself, produce all forms of escape. Lesion experiments also support the involvement of other cells in escapes. In goldfish, electrolytic removal of the Mauthner cell yielded no effect on the behavior, other than a small increase in latency to response (Eaton et al., 1982). These observations led researchers to postulate the existence of parallel pathways, acting along with the Mauthner cell during escapes (Eaton and DiDomenico, 1985; Metcalfe et al., 1986; Foreman and Eaton, 1993). The obvious candidates for these pathways were the Mauthner-like segmental homologs MiD2cm and MiD3cm. Foreman and Eaton (1993) suggested that differential activity of the cells in the Mauthner array (Mauthner, MiD2cm, and MiD3cm) controls the magnitude of the escape. Activity in all three cells would excite more inter- and motoneurons, leading to a larger turn, whereas activity in only one or two cells would excite fewer downstream neurons, leading to a smaller turn.

The proposal of Foreman and Eaton (1993) was supported by our previous functional imaging studies in zebrafish, which showed that sensory stimuli known to elicit different forms of escape behavior also produce different patterns of activation in the Mauthner array (O'Malley et al., 1996). These studies took advantage of the transparency of zebrafish larvae and used a calcium indicator to image the activity of the Mauthner cell, MiD2cm, and MiD3cm during escape responses. As predicted in the Foreman and Eaton model, all three homologs were active during escapes elicited by stimuli to

*To whom correspondence should be addressed (e-mail: jfetcho@neurobio.sunysb.edu).

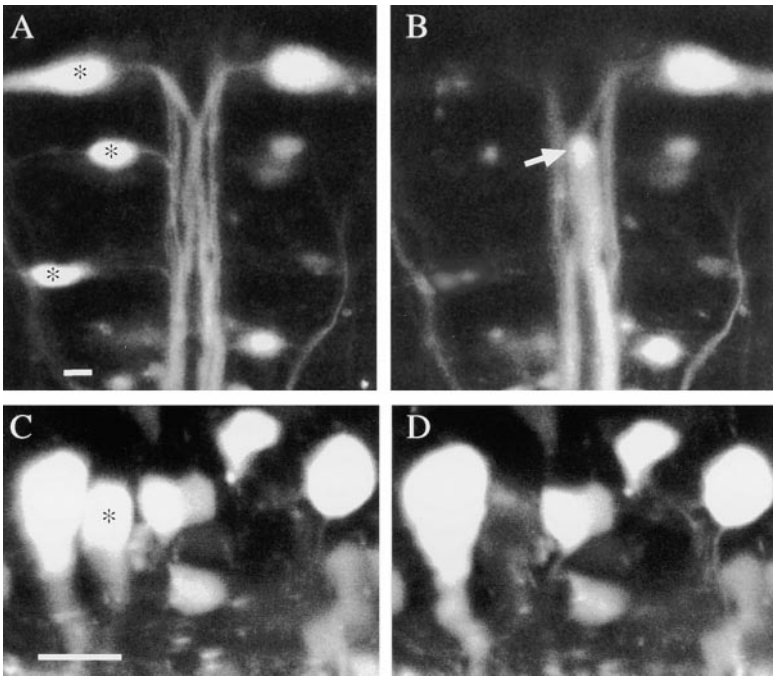

Figure 1. Examples of Ablations

(A and B) A Mauthner array before (A) and the day after (B) laser killing of Mauthner, MiD2cm, and MiD3cm. Images show the hindbrain viewed in horizontal section, with rostral at the top.

(A) Prior to the lesions, there is bilateral labeling of hindbrain neurons with the large, bright somata of the two Mauthner cells on the left and right sides at the top (the asterisk on the top left marks the Mauthner cell on that side). Below the Mauthner cell on the left side are the MiD2cm and MiD3cm cells, also marked by asterisks.

(B) After killing the cells marked by the asterisks in (A), only minor debris is evident where their somata were prior to the lesion. The swollen axon of the ablated Mauthner cell remains and terminates abruptly (arrow) near where it once crossed toward the ablated soma.

(C and D) A cluster of motoneurons in spinal cord before (C) and immediately after (D) laser illumination of the cell marked by an asterisk. The laser is very selective, with only the targeted cell affected by the illumination; immediately adjacent cells retain their fluorescence.

Scale bars, 10 μm.

the head, while only the Mauthner cell was active during escapes elicited by stimuli to the tail. These correlations between neural activity and behavior suggested that cells in the Mauthner array might generate different forms of escape movements but offered no causal links between the neurons and the behavior.

The transparency of zebrafish larvae offered us the opportunity to conclusively link neurons and behavior by examining the consequences of laser ablation of neurons in the Mauthner array. Toward this end, we developed a noninvasive approach for killing single cells that takes advantage of the relative phototoxicity of the dyes we use for calcium imaging. The targets we chose for ablation were the Mauthner cell alone and the entire array, as these sets represent the extremes of activity patterns observed in the imaging studies. Based upon the functional imaging work, our predictions were that killing all three cells in the Mauthner array would remove the ability of the fish to produce high-performance escape turns to both head and tail stimuli, whereas ablating just the Mauthner cell would have a greater effect on turns in response to tail-directed than to head-directed stimuli. The results from killing all three cells in the array matched our predictions. The Mauthner lesions, while partially supporting our predictions, produced unexpected results that allow us to resolve paradoxical observations from previous studies. Our results provide direct support for the idea that repeated hindbrain neurons form functionally related groups.

Results

Specificity and Effectiveness of Lesions

The indicator dyes typically used for visualizing cell activity have adverse affects on the cells when exposed to intense light. We observed such effects in our previous calcium imaging of neurons in zebrafish (Fetcho et al., 1998) and set out to determine if this phototoxicity could be used as a reliable method of killing single cells in zebrafish larvae. Targeted cells were labeled by retrograde uptake after injection of a fluorescent indicator, calcium green dextran (CGD), and identified by position and morphology (Kimmel et al., 1982; Metcalfe et al., 1986) on a confocal microscope. The laser was then focused and maintained at highest intensity on the center of a labeled cell. This led to an immediately noticeable decrease in fluorescence of the cell that was likely due to bleaching of the indicator. A day later, the fluorescent cell body was no longer evident in confocal images, suggesting cell death.

In the current work, a major concern was to identify an accessible and reliable indicator that a cell was indeed successfully killed by this illumination. Because larval zebrafish are transparent, we can view the effects of the photoablation directly in confocal optical sections. The most dramatic examples of the effectiveness of the approach were seen in lesions of the Mauthner cell (Figures 1A and 1B) because its large axon was easily identifiable, even without the cell body. In these cases, optical sections 24 hr after ablations revealed a swollen, truncated axon stump of the Mauthner cell leading toward the original position of the soma (Figure 1B). Survival of the Mauthner axon after somatic lesions has been reported before (Eaton et al., 1982; DiDomenico et al., 1988). We found that a swollen, abruptly terminating Mauthner axon stump was always associated with the loss of a fluorescent soma. In about 25% of the ablation attempts, the Mauthner cell body was fluorescent after 24 hr, with an intensity that was higher than that immediately after the attempted ablation. In these cases, the axons of the cells always looked normal and the ablations were obviously unsuccessful. We suspect that the

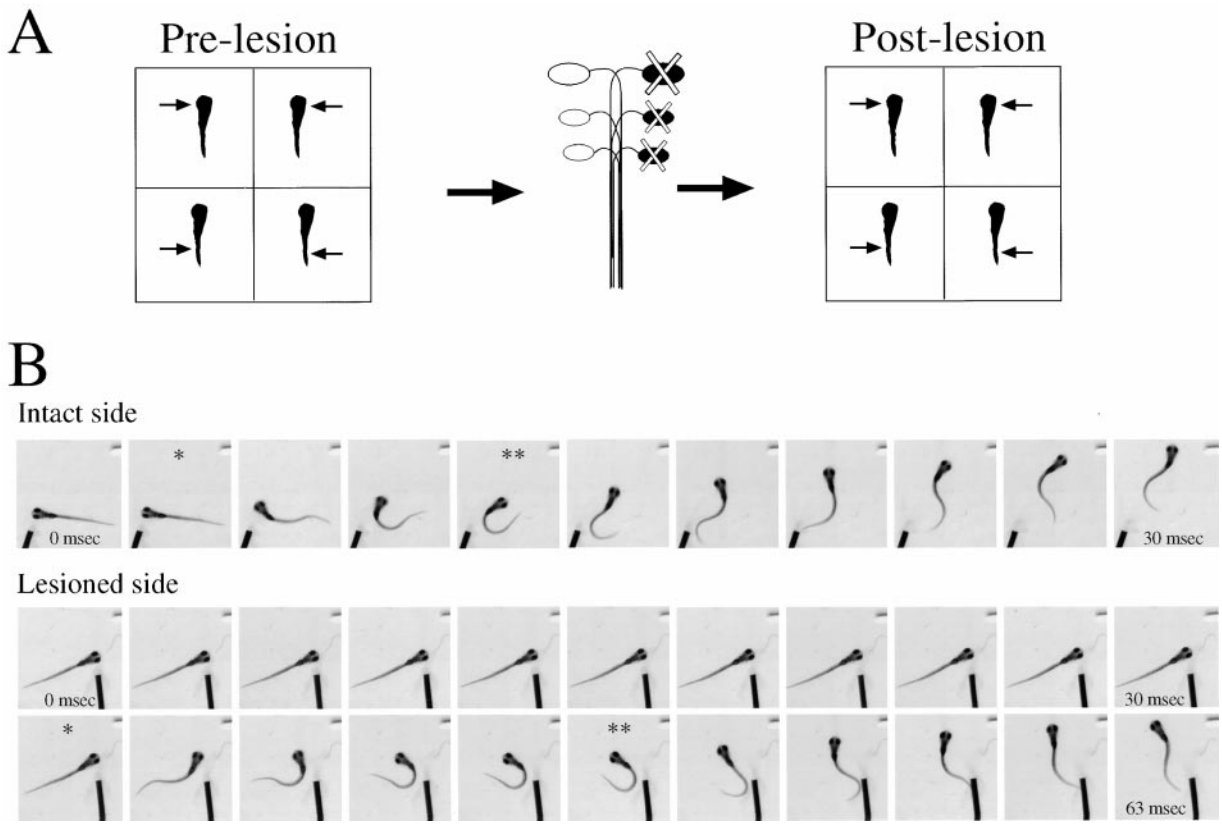

Figure 2. Behavioral Trials

(A) Design of the experiments. Prelesion trials were collected by stimuli in each quadrant on successive trials (left); then, the targeted cells were lesioned (middle); finally, postlesion trials were collected (right).

(B) Examples of two successive escape responses in an array-lesioned fish following stimuli on the intact side (top) and lesioned side (bottom). Frames start when the water pulse contacts the head of the fish. For each trial, a single asterisk marks the initiation of response. The initial movement is difficult to detect in the side-by-side view of the frames shown here but is evident when observed in video clips and on plots of angular velocity. A double asterisk marks the frame of the maximal bend. Note that the response initiated from the lesioned side does not begin until the response from the intact side is complete. The time from the start of the bend to the maximal bending is longer on the lesioned side. Images were collected at 1,000 frames/s, and every third frame is shown (3 ms between frames).

fluorescence intensity recovered because dye that was bleached out of the soma during the attempt to ablate the cell was replaced by dye from the intact axon. The one-to-one correlation between swollen axon stumps and loss of fluorescence in the soma supports the conclusion that the loss of fluorescence (after 24 hr) is due to somatic death.

This conclusion is also supported by experiments in which we viewed cells under differential interference contrast (DIC) optics shortly after exposure to the laser. Targeted cells showed clear indicators of necrosis—the formation of large vacuoles and a more pronounced outline as the cell membrane begins to pull away from its neighbors. These effects were always associated with a loss of fluorescence the next day, again supporting the conclusion that this loss is a reliable indicator of cell death.

To demonstrate further that the loss of fluorescence was not simply due to photobleaching, we simultaneously labeled spinal neurons with Texas red ($\lambda_{ex} = 568$) and CGD ($\lambda_{ex} = 488$) so that cells could be lesioned by excitation of the former and their status monitored with the latter. Cells were targeted with the confocal laser until Texas red fluorescence was reduced to background levels. While these cells were still visible with CGD shortly following the exposure, they were no longer visible with either dye after 24 hr and beyond. Cells not subjected to intense illumination remain fluorescent for weeks. These results suggest that the absence of fluorescence is not due simply to photobleaching but to cell death. Thus, morphological evidence of degeneration in fluorescence and DIC as well as double-labeling experiments all indicate that the loss of fluorescence after 24 hr is a reliable indicator of cell death.

The amount of illumination time required to kill a cell varied with cell size and location. The relatively small and exposed motoneurons in the spinal cord (Figures 1C and 1D) required less than 1 min, while the much larger cells of the Mauthner array deep in the hindbrain (Figures 1A and 1B) required 10–12 min. In the spinal cord, the success rate was close to 100%. In the hindbrain, where the cells are much deeper and occasionally occluded by pigment, the success rate dropped to about 75%. It is possible that some targeted neurons that were

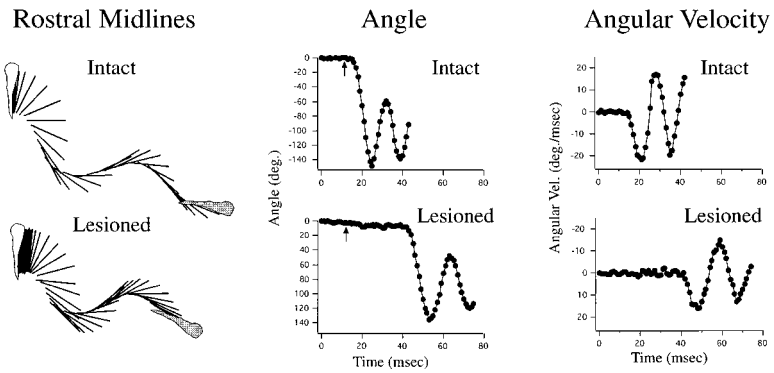

Figure 3. Kinematic Analysis of Escape Trials

Rostral midline plots of an array-lesioned fish (same trials as in Figure 2) show the position of the fish in space over time. Midlines are shown for all frames collected, with 1 ms between lines. Both trials are shown as if the fish were turning to the right to allow easy comparison; they were, however, produced in response to stimuli on opposite sides of the head of the same fish. The stimulus on the intact side leads to a short-latency, rapid turn away. Following a stimulus on the lesioned side, the fish remains still (except for a slight drifting to the right from the push of the water pulse) for much longer than on the intact side and then turns away more slowly, as shown by the more closely spaced lines. The right side shows this quantitatively in plots of the angle turned and the angular velocity of the turn on intact and lesioned sides. The frame in which the stimulus arrives is marked by an arrow on the angle plots.

still fluorescent after 24 hr were damaged, but we did not use these animals in our studies.

Laser illuminating unlabeled fish for the same time periods and in the same regions of the brain as labeled fish did not produce the behavioral effects observed after illuminating labeled cells. This indicates that the lesions were not a direct effect of the laser light, but depended on interactions of the light with the dye in the labeled cells.

These photoablations are highly specific. This is best demonstrated in clusters of spinal motoneurons. A single cell can be targeted in the midst of near neighbors (Figure 1C). Neighboring cells retain their fluorescence both immediately and 1 day after lesioning (Figure 1D). In addition, in calcium imaging studies similar to O'Malley et al. (1996), we found that neurons that respond during escapes retain that ability after lesioning of adjacent cells (data not shown). Thus, this technique is effective, minimally invasive, and highly specific compared to ablation procedures previously used for behavioral studies in vertebrate systems.

Behavioral Experiments

In response to a pulse of water on one side, fish perform a large, fast turn away from the stimulus, followed by a counterbend and further high-speed swimming. To expedite analysis of this escape response, we wrote a program in Labview that automatically tracked the fish and generated plots of several kinematic parameters for each trial. We focused our analysis on the performance of the initial turn in the escape because previous data suggested that the Mauthner array is important for generating the high-performance movements during this turn. Several features of the initial turn were studied: the latency to its initiation (time from the contact of the pulse of water to the beginning of movement), the maximum angle of the turn, its peak angular velocity, and its duration. Two classes of responses—nonescape turns that

Table 1. Means and Standard Errors for Kinematic Parameters

	Array Lesions							
	Head Stimulus				Tail Stimulus			
	Prelesion		Postlesion		Prelesion		Postlesion	
	Lesioned	Intact	Lesioned	Intact	Lesioned	Intact	Lesioned	Intact
Latency (ms)	3.8 ± 0.1	3.1 ± 0.1	43.1 ± 2.2	4.4 ± 0.6	6.2 ± 0.3	8.2 ± 0.5	51.3 ± 3.0	12.7 ± 1.5
Duration (ms)	7.9 ± 0.1	8.0 ± 0.1	17.2 ± 1.2	9.4 ± 0.2	7.3 ± 0.2	7.2 ± 0.2	13.5 ± 1.0	9.1 ± 0.5
Velocity (°/ms)	23.7 ± 0.3	21.3 ± 0.6	14.2 ± 0.7	19.6 ± 0.7	21.5 ± 0.4	21.3 ± 0.5	13.0 ± 0.7	17.4 ± 0.8
Angle (°)	128.7 ± 2.5	117.5 ± 2.1	118.4 ± 4.8	127.4 ± 5.6	108.7 ± 2.0	111.6 ± 2.1	89.9 ± 6.3	96.1 ± 5.5
	Mauthner Cell Lesions							
	Head Stimulus				Tail Stimulus			
	Prelesion		Postlesion		Prelesion		Postlesion	
	Lesioned	Intact	Lesioned	Intact	Lesioned	Intact	Lesioned	Intact
Latency (ms)	3.9 ± 0.2	2.7 ± 0.3	4.6 ± 0.3	4.5 ± 0.5	5.5 ± 0.2	8.1 ± 0.8	37.9 ± 6.2	8.5 ± 0.8
Duration (ms)	8.4 ± 0.1	8.4 ± 0.2	8.9 ± 0.3	9.0 ± 0.5	7.6 ± 0.2	7.3 ± 0.1	9.8 ± 0.8	8.1 ± 0.4
Velocity (°/ms)	24.5 ± 0.5	23.6 ± 0.7	22.3 ± 0.6	21.4 ± 0.3	22.1 ± 0.5	22.6 ± 0.6	17.0 ± 0.7	20.8 ± 0.4
Angle (°)	137.1 ± 4.2	128.5 ± 3.8	132.8 ± 5.8	135.5 ± 6.6	116.8 ± 1.9	112.9 ± 2.7	99.9 ± 4.1	112.4 ± 3.4

The means and standard errors for latency, maximum turn angle, peak angular velocity, and initial turn duration are presented for array lesions (top) and Mauthner cell lesions (bottom). As in Figures 4 and 6, Table 1 is arranged to allow for comparisons between different categories. Note that the prelesion values for the (to be) lesioned and intact sides are generally symmetrical. Exceptions are discussed in the text. The values for the array lesions are calculated from 18 trials (3 trials for each stimulus from each of 6 fish). Those for the Mauthner cell lesions are from 15 trials (3 trials for each stimulus from each of 5 fish).

we call scoots, and turns toward the stimulus—were not included in the data set. A more detailed account of the basis for excluding them is presented in the Experimental Procedures.

A brief account of the experimental design (Figure 2A) is presented here to aid in the interpretation of the results. Larval fish were injected with CGD, and the cell labeling was verified by confocal microscopy. The day after the labeling injection, prelesion behavioral trials were collected at 1000 frames/s for each fish for detailed kinematic analysis (Figure 3). The stimulus was delivered to one of four quadrants on successive trials—left head, right head, left tail, or right tail (Figure 2A). The next day, the targeted neurons—either the Mauthner cell alone or all three array cells—were lesioned on one side of the fish. Postlesion behavioral trials were then collected the day after the lesions in the same manner as described for prelesion trials (Figure 2B). Lastly, the animals were remounted and examined under the confocal, in order to directly verify that the lesioned cells were missing in optical sections of the hindbrain.

A couple of aspects of this approach might lead to behavioral deficits not specific to the lesions. First, the injection of dye to fill the cells for ablation could result in changes in performance. It might, for example, introduce small asymmetries between the two sides not present in uninjected fish. Second, manipulations of the fish, particularly the embedding in agar, were physically demanding to the delicate larval zebrafish and might also result in nonspecific changes in performance. Therefore, we anticipated general nonspecific effects as well as slight asymmetries prior to lesions. The experiments were designed to control for these concerns by allowing us to make two sets of comparisons. We could compare the performance of the same animals before and after lesions. The expectation was that pre- versus postlesion comparisons should reveal large changes on the lesioned side but not on the intact side. Any changes of the intact side could be attributable to nonspecific effects on the fish. We could also compare the two sides of the fish after the lesions, with the expectation that the lesion would introduce a large asymmetry between the two sides. Any observed changes could be confidently attributed to the lesion if we saw both a significant change on the lesioned side relative to its performance prelesion and a coincident, significant asymmetry in performance between the two sides of the fish after the lesion.

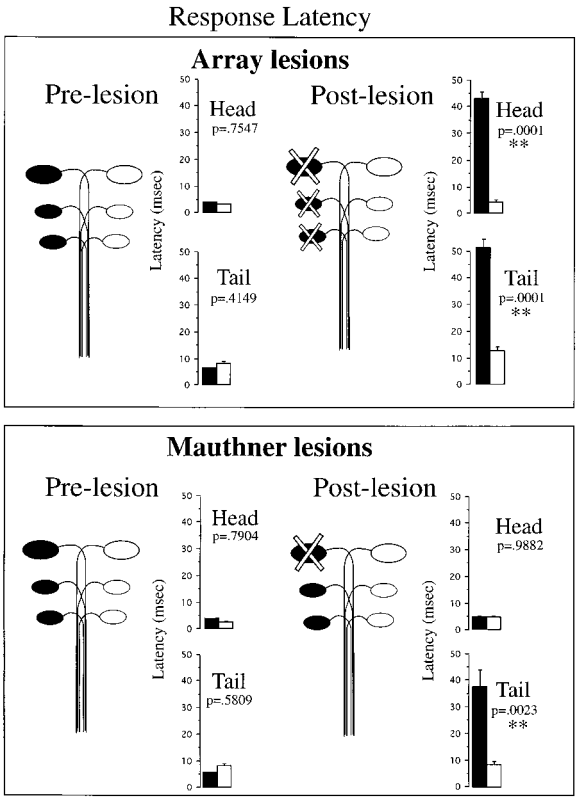

Figure 4. Effects of Lesions on Response Latencies

(Top) Latency to response before and after lesions of the entire Mauthner array (Mauthner, MiD2cm, and MiD3cm). The left side shows the histograms of mean latency for stimuli on the two sides of the head (top) or tail (bottom) prior to the lesions. The histogram bars on the side to be lesioned are in black. Prior to lesioning, the latencies are short (4 ms for head stimuli, slightly longer for tail) and nearly symmetrical on the two sides. The right side shows similar histograms for the two sides after the lesion. The latency on the lesioned side increases dramatically after the lesion to over 8 times its prelesion value, whereas the intact side changes very little.

(Bottom) Histograms for lesions of the Mauthner cell alone in the same format as the top panel. In these, the response latencies increased on the lesioned side for responses to tail stimuli, but did not change for head stimuli. The histograms for array lesions show means ± SEM for 18 trials (3 trials for each stimulus from each of 6 fish). Those for Mauthner lesions are from 15 trials (3 trials for each stimulus from each of 5 fish). The p values report the significance levels for ANOVA contrasts between the two sides of the fish before and after lesions. Asterisks mark those cases with significant ($p < 0.05$) asymmetries between responses to stimuli on opposite sides.

Prelesion Differences in Escapes to Head and Tail Stimuli

Prior to lesions, the escapes produced by water pulses directed at the head differed from those in response to tail stimuli. Head escapes were faster and larger, and they had a shorter latency and a longer duration (Table 1) than tail escapes. The differences in angular velocity and angle turned were statistically significant ($p < 0.05$), and the duration and latency differences were nearly so. In pilot experiments, more robust differences between head and tail escapes were seen in response to taps on the head versus tail from a piezoelectrically driven glass probe. The water pulses are a weaker and probably less directional stimulus than taps, but we chose to use water as our stimulus because repeated taps on the head of the fish were detrimental to the animal's escape performance.

Effects of Lesions on Response Latency

The lesions had the most dramatic effects on the latency to respond to the stimulus. In the prelesion trials, the average latency for head-directed stimuli was 3.4 ms; that for tail-directed stimuli was 7.0 ms. In animals in which all three homologs were killed, the latency to respond to head-directed stimuli on the lesioned side increased 10-fold, from an average of 3–4 ms before lesion to over 40 ms afterward, with little change on the

unlesioned side (Figure 4, top; Table 1). There was also a very significant asymmetry between the two sides after the lesion. A similarly dramatic increase and asymmetry in latency was seen for tail responses after array lesions (Figure 4, top; Table 1).

Figure 2B shows frames taken from two successive behavioral trials of an array-lesioned fish. In the first trial, the stimulus was delivered to the intact side; in the second, to the lesioned side. Frames were collected at 1 ms increments, but only every third frame from the collected sequence is shown (3 ms between frames). An asterisk denotes the initiation of response. Note that the response on the lesioned side did not begin until frame 12 (33 ms). By this time on the intact side, the fish was well into its fourth bend and far from the stimulus site. The lesion effect on latency was also seen in the quantitation of movement in these trials (Figure 3). These array-lesioned fish can still turn away from the squirt, but typically do not even begin to do so until after a normal escape response would be complete. Thus, both the short-latency initial turn and the counter turn of the escape are missing in the lesioned fish. Since the ablated cells are thought to generate the initial turn, the absence of a counter turn suggests that its production is contingent upon the preceding initial turn.

The results for lesions of the Mauthner cell alone were somewhat more complicated. These ablations left latencies to head-elicited responses unchanged but resulted in a significant increase in latencies to tail-elicited responses (Figure 4, bottom). However, the effects were not as robust as those obtained by killing the entire array. Figure 5 shows histogram plots of response latency for all of the postlesion trials, both array and Mauthner cell lesions. For array lesions, the effects on latency were so dramatic that the values for intact versus lesioned sides were completely nonoverlapping for head stimuli (Figure 5A) and largely so for tail stimuli (Figure 5B). While lesions of the array eliminated all short-latency responses to tail-directed stimuli, lesions of the Mauthner cell alone resulted in a broader spectrum of latencies (Figure 5D). Most responses had long latencies like those following array lesion (over 20 ms), but some of the shortest-latency responses (under 10 ms) still occurred.

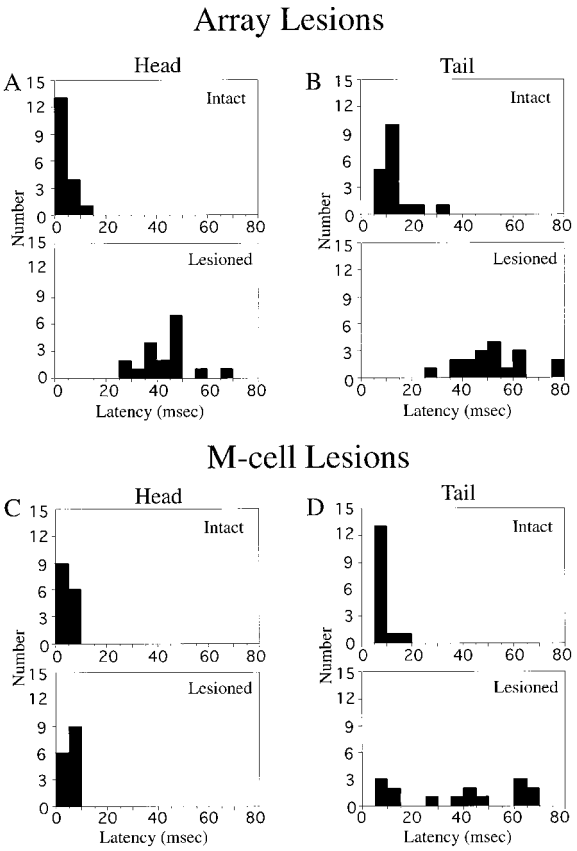

Figure 5. Histograms of the Latency Values from Individual Trials

Each pair of histograms (A–D) compares latency on intact and lesioned sides. (A) and (B) show the effects on latency to response for head and tail stimuli after lesions of the array. (C) and (D) show effects on latency for head and tail stimuli after Mauthner lesions. Lesions of the array removed all high-performance turns, such that the latencies for head-elicited responses on intact and lesioned sides are completely nonoverlapping (A) and the values for tail-elicited responses are largely so (B). Latencies to head-elicited responses after Mauthner lesions were unchanged (C). Lesions of the Mauthner cell produced a broad distribution of tail-elicited turn latencies ([D], bottom), which included some of the shortest-latency turns and many that were longer than those on the intact side ([D], top). The histograms include latencies from all trials in all fish studied (n = 18 trials in each histogram for array-lesioned fish and 15 trials in each histogram for Mauthner-lesioned fish).

Effects of Lesions on Maximum Turn Angle

The lesions had the least dramatic and consistent effects on the maximum angle of the initial turn (Figure 6, turn angle). Before the lesions, the average maximum turn angles in response to head-directed stimuli were 128°; those to tail-directed stimuli were 112°. There was an asymmetry between the two sides before the lesion in one group (head stimuli in array lesions) that was likely a consequence of the labeling injection, since we did not observe such asymmetries in uninjected fish. In animals in which all three homologs were killed, there was a general, small decrease in maximum turn angle in escapes elicited from the lesioned side, but there were not significant asymmetries between lesioned and unlesioned sides after killing cells (Figure 6, turn angle; Table 1). Because the array lesions did not produce both a change on the lesioned side and the development of a significant postlesion asymmetry, we could make no strong conclusions regarding the affects of array lesions on turn angle. Photoablation of the Mauthner cell alone had no effect on head-elicited responses but led to a small but significant ($p = 0.0268$) decrease in angle for tail-elicited responses on the lesioned side as compared to the intact one. These results indicate that while the Mauthner cell and its homologs may contribute slightly, the control of maximum turn angle can largely be determined independently of the Mauthner array.

Effects of Lesions on Angular Velocity

The lesions had clear effects on the angular velocity of the turn (Figure 6, angular velocity), with the pattern of effects very similar to that seen for the latency of the response. Before the lesions, the average peak angular velocity of turns in response to head-directed stimuli

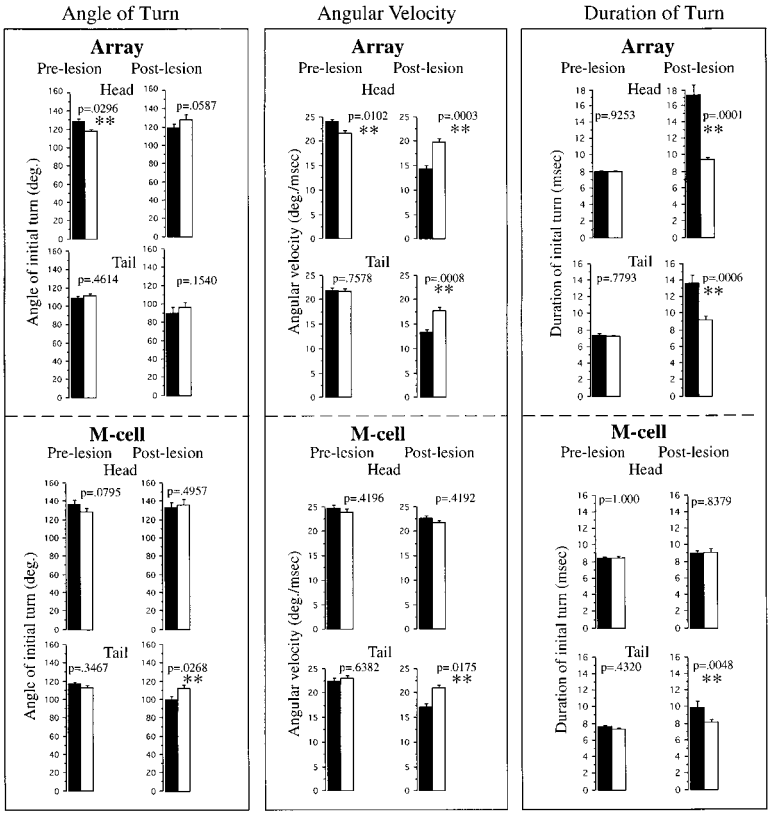

Figure 6. Effects of Lesions on Turn Angle, Angular Velocity, and Duration of the Turn

Histograms of mean values (± SEM) for each kinematic parameter in the same format as those shown for latency in Figure 4. The values for array lesions are in boxes on the top; those for Mauthner (M-cell) lesions are on the bottom. Each box contains histograms for opposite sides of the fish in response to head (top) and tail (bottom) stimuli pre- (left) and post- (right) lesions. The lesioned side is in black in both pre- and postlesion histograms. Bottom panels show the same for lesions of the Mauthner cell alone. The p values for ANOVA contrasts between measurements from opposite sides of the fish are listed, with those pairs showing a significant ($p < 0.05$) difference marked with asterisks. Further details are in the text.

was 23.2°/ms; that to tail-directed stimuli was 21.8 ms. In the array-lesioned group, there was an asymmetry between the two sides in response to head stimuli prior to lesions (likely due to the labeling injection), but the other prelesion results showed good symmetry between sides before the lesion. Killing all three homologs led to a large, significant decrease in angular velocity (to 13°–14°/ms) on the lesioned side for both head- and tail-elicited responses. There were smaller decreases in performance on the intact side after lesion that we attribute to nonspecific effects. However, the large change on the lesioned side led to the introduction of an obvious and significant asymmetry between the two sides after the lesion (Figure 6, angular velocity; Table 1). Photoablation of the Mauthner cell alone resulted in a significant ($p = 0.0175$) decrease in angular velocity for tail-elicited responses but had no effect on head-elicited responses. Thus, killing all three cells dramatically slowed the turn in response to both head and tail stimuli, whereas killing the Mauthner cell alone only slowed tail responses.

Effects of Lesions on Duration of Initial Turn

The previous sections reveal that after array lesions, the fish turn more slowly, but to about the same extent. Thus, one might expect that they should be taking a significantly longer time to complete the turn. This is indeed what we found (Figure 6, duration). Before lesions, there was excellent symmetry in the duration of the turns to both sides. Head turns averaged 8.2 ms; tail turns, 7.3 ms. Killing all three homologs doubled the duration of turns on the lesioned side for both head- (17 ms) and tail-elicited responses (13.5 ms), with only small changes on the intact side. This produced a significant asymmetry between the two sides after the lesion (Figure 6, duration; Table 1). Photoablation of the Mauthner cell alone resulted in a smaller but significant ($p = 0.0048$) increase in turn duration for tail-elicited responses but had no effect on head-elicited responses. Again, the pattern of these changes was similar to those seen for latency and angular velocity.

Discussion

We set out to evaluate the role of the Mauthner array in generating escape responses by examining the behavioral consequences of killing these cells. The Foreman and Eaton model (1993) proposed that the array cells contribute differentially to control the strength of the motor output. The Mauthner cell alone mediates tail-elicited responses, resulting in a shallower bend, while all three homologs are involved in head-elicited responses, resulting in a deeper bend. Using calcium imaging in larval zebrafish, O'Malley et al. (1996) reported that the activity patterns of the Mauthner array match this model. Our lesion results now provide a causal link between these neurons and behavior. Lesions of the Mauthner array resulted in the elimination of high-performance escape responses to both head- and tail-directed stimuli, as measured by latency to response, angular velocity, and turn duration. Lesions of the Mauthner cell alone had significant, similarly detrimental effects on tail-elicited responses, while head-elicited responses appeared unchanged. Since we have not

done separate lesions of MiD2cm and MiD3cm, we do not yet know their individual contributions to escapes. However, the greater impact of the array lesions support the idea that MiD2cm and/or MiD3cm, like the Mauthner cell, contributes to escape behavior.

These results resolve an apparent paradox in earlier Mauthner lesion studies. Substantial physiological evidence links activity of the Mauthner cell to escape behavior (Zottoli, 1977; Eaton et al., 1981; Nissanov et al., 1990). It was therefore surprising when lesioning studies reported few and inconsistent behavioral changes after killing the Mauthner cell (Eaton and Kimmel, 1980; Kimmel et al., 1980; Eaton et al., 1982). After irradiating zebrafish early in development, Kimmel et al. (1980) found that those larvae that lacked a Mauthner cell also exhibited decreased fast-start performances on the lesioned side. However, irradiation likely led to the removal of other cells, some of which might be involved in escape behavior. In the most cell-specific lesions, Eaton et al. (1982) electrolytically killed the Mauthner cell in adult goldfish and found no effects except a small but significant increase in latency. Since the nature of their stimulus did not allow them to determine where the fish would perceive the stimulus along the rostrocaudal axis, head- and tail-elicited responses were pooled together in their analyses. We now know that lesioning the Mauthner cell alone has no effect on head-elicited escapes but does substantially impair tail-elicited responses. These impairments included large effects on the latency to respond and smaller, though still significant, effects on angular velocity and duration of the initial turn. If head- and tail-elicited escapes were pooled together following Mauthner cell lesions, the unchanged head responses would mask the smaller deficits in angular velocity and duration and reduce the large increases in latency. This may explain why, in their pooled data, Eaton et al. (1982) found only changes in latency following Mauthner cell lesions.

Our observations demonstrate that the Mauthner cell does indeed play an important role in generating escape responses, particularly those elicited by caudal stimuli. While clarifying the role of the Mauthner cell in escape behavior, our observations raise new and interesting questions about the relative contributions of the three homologs in the Mauthner array. Based on the Foreman and Eaton model, we would predict that the removal of any of the three homologs should result in a decrease in head-elicited escape performance. However, removal of the Mauthner cell had no discernible effect on head-elicited responses. This is surprising, given that activation of the Mauthner cell is sufficient to produce a strong bend (Nissanov et al., 1990). These observations highlight the difficulties in making predictions about lesioning experiments in complex systems, where several neurons potentially contribute to a behavior (Eaton and DiDomenico, 1985).

In this particular case, a likely explanation for the apparent lack of effects of Mauthner lesions on head-elicited responses is the behavioral context in which the escapes were elicited. The escapes were produced while the animal was still, instead of while swimming. This allowed us more easily to control stimulus direction and strength but ignored some of the adaptive relevance of the fast-start response. A key function of the Mauthner cell is to insure a powerful bend by overriding other motor programs (Svoboda and Fetcho, 1996). It is possible that MiD2cm and MiD3cm can, by themselves, produce a high-performance escape from rest, when axial motor activity is minimal, but could not do so without the Mauthner cell if there was substantial conflicting motor activity. If this explanation is correct, then Mauthner cell lesions should produce impairments in escapes elicited by head stimuli during swimming.

The Foreman and Eaton model and our previous calcium imaging studies, which showed that the Mauthner cell alone is active in escapes to tail stimuli, led us to predict that ablating the Mauthner cell should remove all high-performance tail-elicited responses. However, even in tail-elicited escapes, we did occasionally observe high-performance responses from the lesioned side after killing the Mauthner cell. One possible explanation for the remaining high-performance turns was that they occurred when the stimulus was more rostral than usual, thereby activating one or both of the remaining homologs. However, there was no correlation between these high-performance responses and the rostrocaudal position of the stimulus. Another possibility is that MiD2cm and/or MiD3cm takes over after Mauthner lesions. The fact that these high-performance responses are completely eliminated in animals where the entire array has been lesioned supports a role for MiD2cm and/or MiD3cm in the production of these responses after Mauthner lesions. Functional substitution by MiD2cm and MiD3cm could be revealed by calcium imaging if these cells, which do not respond to tail-directed stimuli in intact fish, do respond to tail-directed stimuli after Mauthner lesions.

Our observations indicate that zebrafish can produce turns of a given amplitude via multiple pathways. While all short-latency, high-performance escapes are removed by lesioning the Mauthner array, the animals are still capable of sensing the stimulus, calculating its direction, and responding with an appropriate amplitude turn, albeit much more slowly and at a very long latency. One can compare the Mauthner array circuit to a reflex pathway, allowing quick and decisive retreat from danger. After its removal, fish can still turn away from stimuli, but they most likely do so via other slower, polysynaptic pathways that require more processing and hence a longer latency to respond. Although these fish can respond with a turn of appropriate amplitude, these slow turns do not even begin until after a normal escape would be complete. Such fish would likely be doomed in a predatory attack.

Our experiments show that the serially repeated reticulospinal neurons in the Mauthner array form a functionally related group. These experiments were possible because zebrafish have relatively few reticulospinal neurons and they form sets of repeated cells with individually identifiable members. However, the overall segmental organization of hindbrain neurons, so obvious in zebrafish, is evident in vertebrates generally (Clarke and Lumsden, 1993). Many of these hindbrain neurons are part of a reticulospinal system that is strikingly similar in fish and mammals (Fetcho, 1992; Lingenhohl and Friauf, 1994). Thus, it seems very likely that segmental functional groups similar to those in zebrafish also exist in other vertebrates.

Laser ablations of single cells, used first to study development (Sulston and White, 1980; Eisen et al., 1989), have proved fruitful for linking neurons to behavior in invertebrate systems (Selverston and Miller, 1980; Chalfie et al., 1985; Bargmann and Horvitz, 1991). Our lesion studies of the Mauthner array in zebrafish extend this approach to the analysis of the behavioral contribution of identified neurons in a vertebrate system. Zebrafish have many other small groups of identifiable neurons in spinal cord and brain whose behavioral roles could be analyzed with this approach. Cell-specific ablations, when combined with the functional imaging at single-cell resolution and the genetic tools also available in zebrafish (Granato et al., 1996; Fetcho and Liu, 1998), should make zebrafish a powerful model for exploring the neural basis of vertebrate behavior.

Experimental Procedures

Larval fish were obtained from laboratory breeding stock. Zygotes were kept in 10% Hank's buffer at 28.5°C until the fish had developed to the point where they could swim in the water column (about 4 days). At this stage, they were moved to room temperature in order to acclimate the fish to the temperature at which the experiments were done (26°C).

Retrograde Labeling

Four- to five-day-old larval zebrafish were anesthetized with 0.02% 3-aminobenzoic acid ethyl ester (MS222). The targeted cells were retrogradely labeled by pressure injection via a glass microelectrode of a 50% solution of CGD (10,000 MW; Molecular Probes, Eugene, OR) in 10% Hank's into the spinal cord (Fetcho and O'Malley, 1995). Injections were targeted to the ventral cord to selectively label Mauthner and its homologs without disrupting more dorsal sensory pathways. Since any injection would disrupt local circuits, injections were also targeted to the most caudal part of the tail and all test stimuli were given rostral to the injection site. After injection, the fish were allowed to recover in 10% Hank's solution containing food (cultured paramecia). Nine to ten hours later, the cell labeling was verified under the confocal microscope. Between four to six of the best-labeled animals were retained in 10% Hank's containing paramecia for behavioral trials.

Confocal Microscopy

The fish were briefly anesthetized in MS222, placed on a cover glass in a petri dish, embedded on their backs in a thin layer of 1.2% agar (Eaton et al., 1984), and screened with confocal microscopy for the desired labeling. Confocal images were obtained by looking into the head of the intact fish using a Zeiss inverted microscope with a 63× water objective and a Zeiss laser-scanning confocal imaging system (LSM 510). Mauthner cells and their homologs were identified by their highly characteristic morphology and position (Kimmel et al., 1982; Metcalfe et al., 1986). The potential for photo-induced damage to the cells during screening was reduced by minimizing the illumination used and increasing the sensitivity of the system (by opening the confocal aperture and increasing gain in the photomultiplier).

High-Speed Recording of Behavior

Labeled fish were placed into individual petri dishes (3.5 cm) filled with 10% Hank's buffer at a depth of 3–4 mm. Escape responses were recorded with a high-speed camera that captures images digitally at 1,000 frames/s (EG&G Reticon, Sunnyvale, CA). At the same time, a slow-speed video camera recorded the entire procedure. In this way, we could verify later which trials were retained digitally and the history of each trial. Escape responses were elicited by a measured pulse of water, delivered from a picospritzer (General Valve, Fairfield, NJ) through a syringe and 2$\hat{7}$ gauge needle cut blunt and bent to about 100°. In order to monitor the stimulus, fast green dye was added to the water at a concentration of 0.05 mg/ml. The needle tip was kept about 0.5 mm from the fish at the time the stimulus was given. A successful escape trial was recorded from the beginning of the trigger to the picospritzer, as indicated by a stimulus indicator—a deflection of a piezoelectric crystal that was wired in parallel with the picospritzer. Typically, the water left the needle tip about 10–14 ms after the crystal deflection and hit the fish about 2 ms after that.

The water pulses were generated by a pressure pulse of 17 psi and 5 ms duration. The pressure was occasionally adjusted in order to achieve a consistent stimulus (as monitored by the speed of exit of the dye) but adjustments did not vary more than ±1 psi. These settings were determined to be the lowest level that can reliably produce an escape response without the water stream disturbing the animal's movements.

Squirting the colored water in front of the fish, so that the animal might see but not feel the stimulus, did not elicit a response. Therefore, we believe the animals are not responding to the visual aspects of the stimulus. The most likely sensory modalities mediating the response are the somatosensory system, the lateral line, or the ear. If the response is visual, our latency measurements should be calculated from the time the dye exits the needle, instead of from the time the water made contact with the fish. This would have added only about 2 ms to our latency data. This small change would not have altered our conclusions about the consequences of lesions, which had large affects on latency.

Stimuli to the head were directed at the ear. Stimuli to the tail were directed caudal to the anal pore but well rostral to the injection site. The order of stimulus presentation was to the left side of the head and then the right, followed by the left side of the tail and then the right. All of the fish in the group were tested for the same quadrant before moving on to the next trial/quadrant. Therefore, each fish rested between trials for an average of around 20 min. Also, each fish was not presented with a stimulus in the same quadrant for well over 1 hr. Such delays should prevent habituation, fatigue, etc. On occasion, a fish either failed to respond to the stimulus, the stimulus missed the fish, the fish gave a premature response, or the fish turned slightly on its side. Only responses that occurred after the stimulus was deployed and in which the fish remained upright throughout the initial bend were analyzed digitally. A minimum of 20 trials were collected per fish (5 trials per quadrant).

In pilot experiments, we elicited escapes by using a glass probe driven by a piezoelectric device to abruptly touch the fish on the head or tail. This produced more robust differences in the form of the escapes to head and tail stimuli than the squirts, but because the taps were more traumatic to the fish we elected to use squirts to obtain the many trials needed for the lesion experiments.

Photoablation of Cells

After prelesion behavioral testing and overnight recovery, the fish were mounted in agar as described above and the target neurons—either Mauthner alone or all three array cells—were reidentified by their position and morphology (Kimmel et al., 1982; Metcalfe et al., 1986). To lesion a targeted cell, the confocal microscope was focused at the highest zoom (Zeiss 63× water 0.9 NA) on the brightest point of the labeled cell, and the cell was exposed to the laser (λ_{ex} = 488) at maximum intensity. To kill the Mauthner cell, exposure for 10 min was usually necessary. The smaller homologs, probably because they contain less dye, required longer exposures of up to 12 min. We checked the region of the illumination to make sure there was no evidence of general tissue damage immediately after the ablation and 2 days later. Exposure for longer than 20 min could lead to tissue damage, so we limited the exposure to well below that duration. Our attempts to use the minimal effective exposure time might explain why not all of our lesion attempts were successful. After exposure to the laser, the fish were transferred from agar into a small petri dish of 10% Hank's buffer containing paramecia and allowed to recover overnight. Following postlesion behavioral trials, the animals were remounted for confocal microscopy in order to verify the success of the lesions and check for peripheral damage.

Data Analysis

Several kinematic parameters of the initial turn of the escape were selected for analysis: the latency to its initiation (time from the contact of the pulse of water to the beginning of the bending movement),

the maximum angle of the turn, its peak angular velocity, and its duration (time from the beginning of movement to the maximum angle). The movements of the fish were analyzed for these kinematic parameters by using a specialized program written in Labview (National Instruments, Austin TX). The analysis was automated; the image of the fish was thresholded and the binary silhouette of the fish was used to determine, via fitting routines, the location of the rostral midline, which does not bend much during the turns. The midline from each successive frame was plotted to give a representation of the animal's movements (Figure 3, top). The program calculated the angle between the position of the midline in successive frames and its original position (Figure 3, middle) and also provided other kinematic data such as the duration of the turn and the angular velocity, which was obtained by differentiation of the curves for turn angle (Figure 3, bottom).

These parameters were then statistically compared using analysis of variance (SuperAnova, Abacus Concepts, Berkeley CA) with repeated measures. We used statistical contrasts in the ANOVA to perform specific comparisons that we identified as the important ones prior to the experiment. These included comparisons of prelesion versus postlesion, intact side versus lesioned side, head versus tail, and lesions of the array versus lesions of the Mauthner cell alone.

Not every trial collected was used in our statistical analysis. Those trials that were omitted fell into two classes: nonescape or scoot responses, and escape responses in which the fish turned toward the stimulus. These classes and the justification for their omission are discussed below. The data presented comprise three trials prelesion and three postlesion (out of five collected in each case) from each quadrant of eleven fish: six fish with array lesions and five with just Mauthner lesions.

In a small percentage (17%) of trials, the fish moves away from the stimulus with a movement that is sufficiently different from an escape response that it can be distinguished visually during the behavior. These responses consist of a very weak turn away from the stimulus, followed by a somewhat larger turn in the same direction, with no evidence of the initial turn/counter turn sequence typical for escapes. This appears visually as a weak scoot away from the stimulus. We analyzed the kinematics of these responses to verify that they were easily distinguishable from escapes. They consisted of an initial very small (about 10°) and slow (less than 4°/ms) turn away, followed after a long (more than 20 ms) pause by another turn in the same direction. This is very different from an escape, which consists of a large, rapid, continuous turn away from the stimulus, followed by a robust counter turn. The scoot responses were seen with the same frequency in prelesion trials and postlesion trials and were, therefore, not a result of cell lesion. Since the scoots were qualitatively different movements from escapes, we did not include them in our analysis.

On occasion, an animal turned toward the direction of the stimulus. This inappropriate response was almost never seen in intact fish but the frequency increased in fish that had been injected (4%) and increased even more in lesioned fish (11%). There was no difference in the frequency of these turns between fish in which the entire array was lesioned and those in which only Mauthner was lesioned. Turns toward the stimulus exhibited a short latency and high angular velocity that is characteristic of responses of intact fish. After lesioning, these turns occurred only when the stimulus was presented on the lesioned side and not when it was presented on the intact side. For these reasons, we believe that these turns were the result of the Mauthner array cells on the remaining, intact side being inappropriately activated. Increased activation of the intact side following unilateral Mauthner cell lesion has been reported previously in goldfish (DiDomenico et al., 1988). Because these inappropriate responses were most likely mediated by the cells on the unlesioned side, they were not included in our analysis.

Acknowledgments

The authors would like to thank Melina Hale for many helpful comments on the manuscript. The work reported here was supported by NIH grant NS26539 (J. R. F.) and a postdoctoral fellowship from the Helen Hay Whitney Foundation (K. S. L.).

Received April 15, 1999; revised May 17, 1999.

References

Bargmann, C.I., and Horvitz, H.R. (1991). Chemosensory neurons with overlapping functions direct chemotaxis to multiple chemicals in *C. elegans*. Neuron *7*, 792–742.

Chalfie, M.J., Sulston, J.E., White, J.G., Southgate, E., Thomson, J.N., and Brenner, S. (1985). The neural circuit for touch sensitivity in *Caenorhabditis elegans*. J. Neurosci. *5*, 956–964.

Clarke, J.D., and Lumsden, A. (1993). Segmental repetition of neuronal phenotype sets in the chick embryo hindbrain. Development *118*, 151–162.

DiDomenico, R., Nissanov, J., and Eaton, R.C. (1988). Lateralization and adaptation of a continuously variable behavior following lesions of a reticulospinal command neuron. Brain Res. *473*, 15–28.

Eaton, R.C., and DiDomenico, R. (1985). Command and the neural causation of behavior: a theoretical analysis of the necessity and sufficiency paradigm. Brain Behav. Evol. *27*, 132–164.

Eaton, R.C., and Emberley, D.S. (1991). How stimulus direction determines the trajectory of the Mauthner-initiated escape response in a teleost fish. J. Exp. Biol. *161*, 469–487.

Eaton, R.C., and Kimmel, C.B. (1980). Directional sensitivity of the Mauthner cell system to vibrational stimulation in zebrafish larvae. J. Comp. Physiol. [A] *140*, 337–342.

Eaton, R.C., Lavender, W.A., and Wieland, C.M. (1981). Identification of Mauthner-initiated response patterns in goldfish: evidence from simultaneous cinematography and electrophysiology. J. Comp. Physiol. [A] *144*, 521–531.

Eaton, R.C., Lavender, W.A., and Wieland, C.M. (1982). Alternative neural pathways initiate fast-start responses following lesions of the Mauthner neuron in goldfish. J. Comp. Physiol. [A] *145*, 485–496.

Eaton, R.C., Nissanov, J., and Wieland, C.M. (1984). Differential activation of Mauthner and non-Mauthner startle circuits in the zebrafish: implications for functional substitution. J. Comp. Physiol. [A] *155*, 813–820.

Eisen, J.S., Pike, S.H., and Debu, B. (1989). The growth cones of identified motoneurons in embryonic zebrafish select appropriate pathways in the absence of specific cellular interactions. Neuron *2*, 1097–1104.

Fetcho, J.R. (1992). The spinal motor system in early vertebrates and some of its evolutionary changes. Brain Behav. Evol. *40*, 82–97.

Fetcho, J.R., and Liu, K.S. (1998). Zebrafish as a model system for studying neuronal circuits and behavior. In Neural Mechanisms for Generating Locomotor Activity, O. Kiehn, R.M. Harris-Warrick, L.M. Jordan, H. Hultborn, and N. Kudo, eds. Ann. NY Acad. Sci. *860*, 333–345.

Fetcho, J.R., and O'Malley, D.M. (1995). Visualization of active neural circuitry in the spinal cord of intact zebrafish. J. Neurophysiol. *73*, 399–406.

Fetcho, J.R., Cox, K.J.A., and O'Malley, D.M. (1998). Monitoring activity in neuronal populations with single-cell resolution in a behaving vertebrate. Histochem. J. *30*, 153–167.

Foreman, M.B., and Eaton, R.C. (1993). The direction change concept for reticulospinal control of goldfish escape. J. Neurosci. *13*, 4104–4113.

Granato, M., van Eeden, F.J., Schach, U., Trowe, T., Brand, M., Furutani-Seiki, M., Haffter, P., Hammerschmidt, M., Heisenberg, C.P., Jiang, Y.J., et al. (1996). Genes controlling and mediating locomotion behavior of the zebrafish embryo and larva. Development *123*, 399–413.

Kimmel, C.B., Eaton, R.C., and Powell, S.L. (1980). Decreased fast-start performance of zebrafish larvae lacking Mauthner neurons. J. Comp. Physiol. [A] *140*, 343–350.

Kimmel, C.B., Powell, S.L., and Metcalfe, W.K. (1982). Brain neurons which project to the spinal cord in young larvae of the zebrafish. J. Comp. Neurol. *205*, 112–127.

Lingenhohl, K., and Friauf, E. (1994). Giant neurons in the rat reticular formation: a sensorimotor interface in the elementary acoustic startle circuit? J. Neurosci. *14*, 1176–1194.

Metcalfe, W.K., Mendelson, B., and Kimmel, C.B. (1986). Segmental homologies among reticulospinal neurons in the hindbrain of the zebrafish larva. J. Comp. Neurol. *251*, 147–159.

Nissanov, J., Eaton, R.C., and DiDomenico, R. (1990). The motor output of the Mauthner cell, a reticulospinal command neuron. Brain Res. *517*, 88–98.

O'Malley, D.M., Kao, Y.-H., and Fetcho, J.R. (1996). Imaging the functional organization of zebrafish hindbrain segments during escape behavior. Neuron *17*, 1145–1155.

Selverston, A.I., and Miller, J.P. (1980). Mechanisms underlying pattern generation in lobster stomatogastric ganglion as determined by selective inactivation of identified neurons. I. Pyloric system. J. Neurophysiol. *44*, 1102–1121.

Sulston, J.E., and White, J.G. (1980). Regulation and cell autonomy during postembryonic development of *Caenorhabditis elegans*. Dev. Biol. *78*, 577–597.

Svoboda, K.R., and Fetcho, J.R. (1996). Interactions between the neural networks for escape and swimming in goldfish. J. Neurosci. *16*, 843–852.

Zottoli, S.J. (1977). Correlation of the startle reflex and Mauthner cell auditory responses in unrestrained goldfish. J. Exp. Biol. *66*, 243–254.